JOURNAL OF GEOPHYSICAL RESEARCH, VOL. 106, NO. E12, PAGES 33,105–33,119, DECEMBER 25, 2001

# The summer 1997 eruption at Pillan Patera on Io: Implications for ultrabasic lava flow emplacement

David A. Williams,[1] Ashley G. Davies,[2] Laszlo P. Keszthelyi,[3] and Ronald Greeley[1]

**Abstract.** Galileo data and numerical modeling were used to investigate the summer 1997 eruption at Pillan Patera on Io. This event, now defined as "Pillanian" eruption style [*Keszthelyi et al.*, this issue], included a high-temperature (>1600°C), possibly ultrabasic, 140-km-high plume eruption that deposited dark, orthopyroxene-rich pyroclastic material over >125,000 km$^2$, followed by emplacement of dark flow-like material over >3100 km$^2$ to the north of the caldera. We estimate that the high-temperature, energetic episode of this eruption had a duration of 52-167 days between May and September 1997, with peak eruption temperatures around June 28, 1997. Galileo 20 m pixel$^{-1}$ images of part of the Pillan flow field show a widespread, rough, pitted surface that is unlike any flow surface we have seen before. We suggest that this surface may have resulted from (1) a fractured lava crust formed during rapid, low-viscosity lava surging, perhaps including turbulent flow emplacement; (2) disruption of the lava flow by explosive interaction with a volatile-rich substrate; or (3) a combination of 1 and 2 with or without accumulation of pyroclastic materials on the surface. Well-developed flow lobes are observed, suggesting that this is a relatively distal part of the flow field. Shadow measurements at flow margins indicate a thickness of ~8-10 m. We have modeled the emplacement of putative ultrabasic flows from the summer 1997 Pillan eruption using constraints from new Galileo data. Results suggest that either laminar sheet flows or turbulent channelized flows could have traveled 50-150 km on a flat, unobstructed surface, which is consistent with the estimated length of the Pillan flow field (~60 km). Our modeling suggests low thermal erosion rates (<0.1 m d$^{-1}$), and that the formation of deep (>20 m) erosion channels was unlikely, especially distal to the source. We calculate a volumetric flow rate of ~2-7 x 10$^3$ m$^3$ s$^{-1}$, which is greater than those for typical Mauna Loa/Kilauea flows but comparable to those for the (1783) Laki eruption and the inferred flow rates of the Roza flows in the Columbia River flood basalts. The differences in ultrabasic eruption styles on Earth and Io appear to be controlled by the different eruption environments: Plumes at sites of ultrabasic eruptions on Io suggest strong magma-volatile interactions on a low-gravity body lacking an atmosphere, whereas the geology at sites of komatiite eruptions on Earth suggest mostly submarine emplacement of thick flows with a pronounced lack of subaerial explosive activity.

## 1. Introduction

In late June 1997 the Galileo spacecraft's solid-state imaging (SSI) system observed a 140-km-high plume eruption over the Ionian volcano Pillan Patera during orbit C9 (Table 1) [*McEwen et al.,* 1998a]. Analysis of SSI and Near-Infrared Mapping Spectrometer (NIMS) data suggested that the materials emplaced during this event had minimum eruption temperatures >1870 K (>1600°C [see *Davies et al.*, this issue]), much hotter than the hottest terrestrial basaltic eruptions. Two and a half months later during orbit C10, Galileo observations showed a new, Arizona-sized diffuse dark deposit around Pillan [*McEwen et al.,* 1998a], and Galileo spectral data suggested that this material included orthopyroxene [*McEwen et al.*, 1998b; *Geissler et al.*, 1999]. *McEwen et al.* [1998b] concluded that the C9 event was consistent with eruption of high-temperature, magnesium-rich ultrabasic silicates. Thus this eruption provided the first evidence for active ultramafic eruptions in the solar system since komatiites were emplaced on Earth [e.g., *Green,* 1975; *Arndt and Nisbet*, 1982]. Using the limited Galileo temperature and spectroscopic data, *Williams et al.* [2000a] identified a possible terrestrial analog composition to the putative Ionian ultrabasic materials, and they used numerical modeling to assess a possible emplacement style of ultrabasic lavas on Io. Since these studies, high-resolution (20 m pixel$^{-1}$) Galileo images were obtained of the 1997 Pillan deposits during orbit I24 (October 1999). These images can be used to further understand the morphology and emplacement style of the Pillan deposits.

In this paper we use the new Galileo images and analyses of other data to study the emplacement of ultrabasic materials at Pillan Patera. First, we review the volcanic history of Pillan and the nature of the 1997 eruption from previous and new Galileo data. Second, we discuss our observations and interpretations of the high-resolution images of the Pillan materials obtained during orbit I24. Third, we discuss new information from these analyses that can better constrain lava emplacement of the putative Pillan flows, and we present new numerical modeling results. Finally, we discuss our insights on the 1997 Pillan eruption and its products from studies of terrestrial komatiites.

[1]Department of Geological Sciences, Arizona State University, Tempe, Arizona.

[2]Jet Propulsion Laboratory, California Institute of Technology, Pasadena, California.

[3]Lunar and Planetary Laboratory, University of Arizona, Tucson, Arizona.



Paper number 2000JE001339.
0148-0227/01/2000JE001339$09.00

**Table 1.** Galileo Orbits Around Jupiter[a]

| Mission | Orbit | Date |
|---|---|---|
| NOM | J0 | Dec. 7, 1995 |
| NOM | G1 | June 29, 1996 |
| NOM | G2 | Sept. 6, 1996 |
| NOM | C3 | Nov. 6, 1996 |
| NOM | E4 | Dec. 18, 1996 |
| NOM | E6 | Feb. 20, 1997 |
| NOM | G7 | April 3, 1997 |
| NOM | G8 | May 7, 1997 |
| NOM | C9 | June 27, 1997 |
| NOM | C10 | Sept. 18, 1997 |
| NOM | E11 | Nov. 7, 1997 |
| GEM | E12 | Dec. 16, 1997 |
| GEM | E14 | March 29, 1998 |
| GEM | E15 | May 31, 1998 |
| GEM | E16 | July 21, 1998 |
| GEM | E17 | Sept. 26, 1998 |
| GEM | E18 | Nov. 22, 1998 |
| GEM | E19 | Feb. 1, 1999 |
| GEM | C20 | May 5, 1999 |
| GEM | C21 | June 30, 1999 |
| GEM | C22 | Aug. 14, 1999 |
| GEM | I24 | Oct. 11, 1999 |
| GEM | I25 | Nov. 26, 1999 |
| GEM | E26 | Jan. 4, 2000 |
| GMM | I27 | Feb. 22, 2000 |
| GMM | G28 | May 20, 2000 |
| GMM | G29 | Dec. 28, 2000 |
| GMM | C30 | May 25, 2001 |
| GMM | I31 | Aug. 6, 2001 |
| GMM | I32 | Oct. 16, 2001 |
| GMM | I33 | Jan. 17, 2002 |
| GMM | A34 | Nov. 5, 2002 |
| GMM | J35[b] | Sept. 21, 2003 |

[a]Orbit letter designates primary remote sensing target: J, Jupiter; I, Io; E, Europa; G, Ganymede; C, Callisto; A, Amalthea. No remote sensing was performed on orbits E5; E13; and C23. NOM, Galileo Nominal Mission; GEM, Galileo Europa mission; GMM, Galileo millennium mission.
[b]Galileo impact into Jupiter.

## 2. Volcanism at Pillan Patera

The volcanic history of Pillan Patera through the Galileo nominal mission (see Table 1) is given by *McEwen et al.* [1998a]. A description of surface changes at Pillan through the Galileo Europa mission (GEM) is given by *Phillips* [2000]. The evolution of thermal emission from Pillan as seen by the Galileo Near-Infrared Mapping Spectrometer (NIMS) is described by *Davies et al.* [this issue]. During the Voyager era, Pillan Patera (Figure 1) appeared to be a simple caldera with no dark features indicative of silicate eruption products [*McEwen*, 1988], and Pillan appeared unchanged between Voyager 2 and Galileo's first orbit (G1, see Table 1) [*McEwen et al.*, 1998a], although SSI detected a hot spot at nearby Reiden Patera during orbit G1. NIMS detected the first hot spot at Pillan during orbits G2-E4 [*Lopes-Gautier et al.*, 1997], and SSI images showed a dark caldera floor in G2 images. The floor had brightened by orbit C3, but this may have been due to fallout from nearby Pele [*McEwen et al.*, 1998a].

Some dark flows are apparent at Pillan in G7 images (April 3, 1997), but there is no evidence of a hot spot (Figures 1 and 2). NIMS observed Pillan during orbit G8 (May 7, 1997), and it recorded evidence of a high-temperature eruption underway. A two-temperature-area model [*Davies et al.*, 1997] fitted to the NIMS data (which cover wavelengths from 0.7 to 5.2 μm) has been used as a metric to understand how the eruption evolved from May 1997 through May 1999. For the G8 data (May 17, 1997), the two-temperature model fit to NIMS spectra yields a high temperature of 1509 ± 78 K (1236 ± 109°C) with an area 0.20 ± 0.06 km$^2$ and a low temperature of 857 ± 18 K (584 ± 18°C) with an area of 31 ± 3 km$^2$ [*Davies et al.*, this issue]. As lava (once erupted) cools rapidly from liquidus or near-liquidus temperatures, the identification of such a high-temperature component indicates that an eruption was in progress where large enough areas at silicate liquidus temperatures were exposed so as to enable detection from a distance of over 950,000 km. The two-temperature fit also sets a lower limit on magma liquidus temperature, in this case, over 1500 K (> 1230°C). This temperature is consistent with high-Mg mafic silicates.

Both SSI and NIMS observed Pillan during orbit C9 (June 28, 1997), in which SSI observed a 140-km-high plume at Pillan [*McEwen et al.*, 1998a]. Applying the two-temperature model to NIMS data revealed a high-temperature of 904 to 987 K (631-714°C) covering 17 to 27 km$^2$ and a low-temperature of 381 to 497 K (108-224°C) covering 519 to 2054 km$^2$ [*Davies et al.*, this issue]. However, the intensity measured by SSI at shorter wavelengths than NIMS indicated that some part of the erupted material was at temperatures in the range 1500-2600 K (~1230-2330°C). This result was the first indication of possible ultramafic temperatures on Io [*McEwen et al.*, 1998b]. These hot areas detected by SSI were so small that NIMS was not sensitive to them. Subsequent fitting of the combined SSI-NIMS C9 data set revealed that the minimum temperature ($T$) at Pillan was 1870 K (~1600°C) [*Davies et al.*, this issue]. The presence of the large plume, along with the identification of areas at high temperatures, suggests that the style of volcanism is vigorous, such as lava fountaining, or turbulent flows, which continually expose new incandescent material [*Davies et al.*, this issue]. The high-$T$ component most likely relates to these areas of newly exposed lava, and the cooler component represents the cooled crust that rapidly forms on exposed lava [*Crisp and Baloga*, 1994; *Davies et al.*, 1997]. From NIMS data the total thermal emission from Pillan reached a peak during C9. Pillan was emitting 3.5 x 10$^{12}$ W, or more than 40 times that emitted by Prometheus [*Davies et al.*, this issue], a constantly active Ionian volcano. Compared to terrestrial volcanoes, the thermal output per unit area at Pillan during C9 (~2 kW m$^{-2}$ [*Davies et al.*, this issue]) is comparable to that emitted from open channel flows at Etna and Krafla [*Harris et al.*, 1997, 2000].

Both SSI and NIMS again observed Pillan during orbit C10 (September 18, 1997). SSI imaged the 400-km-diameter dark diffuse deposit (Figures 1 and 2) around Pillan [*McEwen et al.*, 1998a], which contains a region of very dark materials at its center. The dark diffuse material was interpreted to be silicate pyroclastics, whereas the very dark material was interpreted to be lava flows [*McEwen et al.*, 1998a]. These very dark materials are estimated to be at least 60 km long and up to 60 km wide (Plate 1), with an areal extent of 3100 km$^2$. NIMS two-temperature-area modeling indicated a C10 hot spot with a high temperature of 1321 ± 15 K (1048 ± 15°C), with an area of 1.19 ± 0.18 km$^2$ and a low temperature of 470 ± 2 K (197 ± 2°C), with an area of 335 ± 17 km$^2$ [*Davies et al.*, this issue]. The relatively large area at 1321 K suggests that part of the volcano was still very active. By C10 the NIMS-derived total thermal emission had decreased from the C9 peak by a factor of 3 to 1 x 10$^{12}$ W, still greater than that seen at many other hot spots on Io [*Davies et al.*, this issue]. An additional SSI eclipse observation from C10 showed two hot spots at Pillan, and *McEwen et al.* [1998a] suggested that they might correspond with the vent and toe of a 75-km-long dark flow-like feature within the dark diffuse deposit northeast of Pillan.

SSI made two eclipse observations of the Pillan region during orbit E11 (November 7, 1997), and analysis suggests that

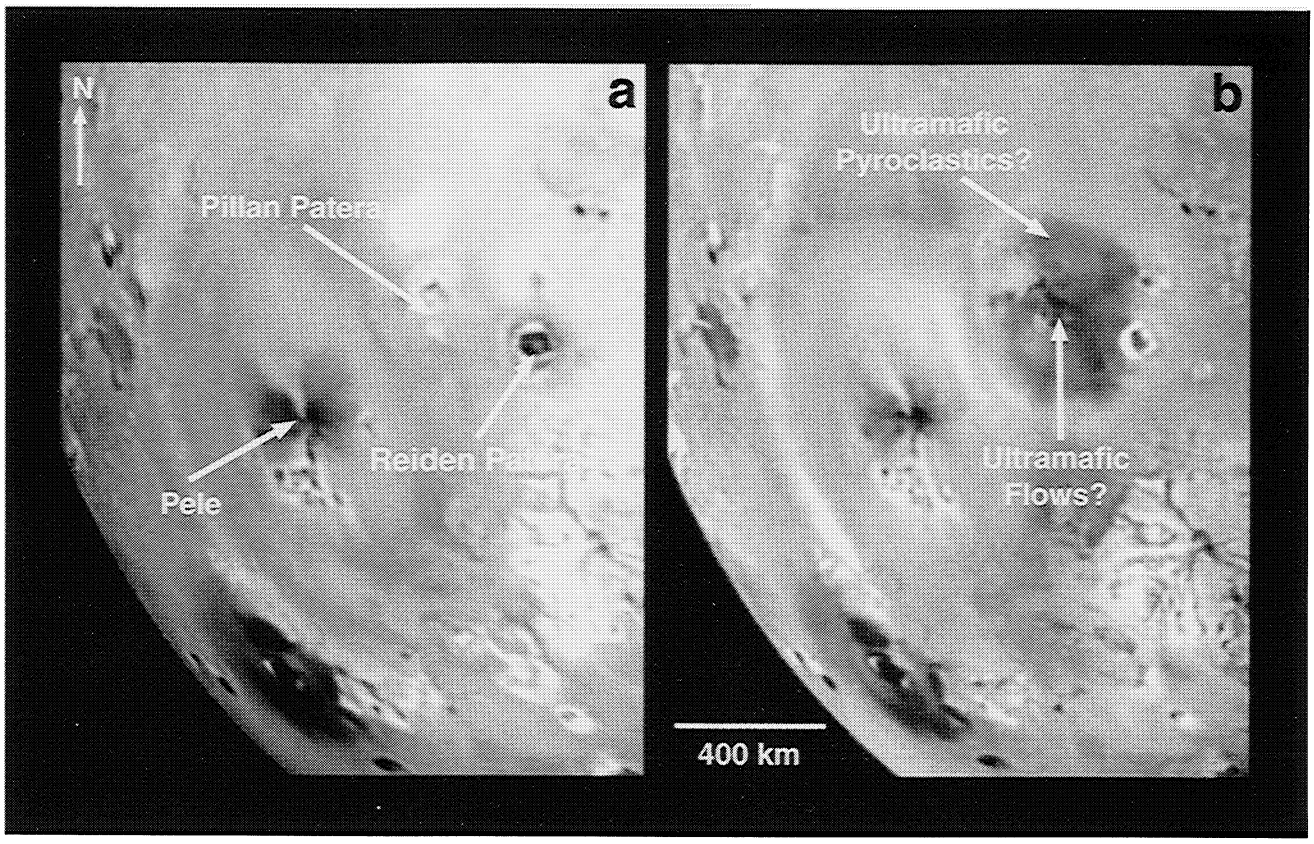


**Figure 1.** Galileo images of the Pele-Pillan region, taken during orbits (a) G7 (April 1997) and (b) C10 (September 1997). The large dark spot in Figure 1b is ~400 km in diameter and may consist of ultramafic pyroclastics and lava flows from the very high temperature 1997 eruption at Pillan. North is to the top of the images. These images were taken at resolutions of 6 km pixel$^{-1}$ for Figure 1a and 5 km pixel$^{-1}$ for Figure 1b. Galileo press release PIA00744, modified from *Williams et al.* [2000a].

there may have been two hot spots separated by ~2° of latitude (~380 km). Both hot spots had high temperatures, >1450 K (>1180°C) over an area of 0.0012 km$^2$ at the northern hot spot and >1300 K (>1030°C) over an area of 0.029 km$^2$ at the southern hot spot [*McEwen et al.,* 1998b]. During the Galileo Europa mission the Pillan region was observed by SSI or NIMS during orbit E14 (March 1998), E15 (May 1998), C20 (May 1999), C21 (June 1999), I24 (October 1999), and E26 (December 1999). The E14 images [see *Keszthelyi et al.,* this issue] show that in addition to the flows observed during C10 outside of the Pillan caldera, other flows may have flooded into the now darkened caldera (an additional 2500 km$^2$ of flows). There was a steady decrease in thermal output at Pillan as determined from NIMS data from 8 x $10^{11}$ W during orbit E15 to 5 x $10^{11}$ W during orbit E16 to 3 x $10^{11}$ during orbit C20, as the eruption died down and the flows cooled. The post-E14 SSI images show that the dark diffuse deposit around Pillan is slowly being buried by red (sulfurous?) material from Pele and by dark (silicates?) and bright (sulfur and $SO_2$?) materials from two unnamed hot spots east of Pillan. As of April 2001, no further plumes were detected at Pillan Patera. A hot spot was detected apparently at Pillan in an Io eclipse movie made by the Cassini spacecraft during its December 2000 flyby.

The volcanic activity at Pillan Patera during the 1997 eruption can be summarized as follows: (1) The volcanoes in the Pillan region were intermittently active during 1996 and early 1997. (2) A major eruption had started by G8 (May 1997) with emplacement of high-temperature, possibly ultrabasic materials. (3) The eruption rose to a peak around June 28, 1997 (orbit C9), and included both high-temperature (>1870 K or 1600°C), effusive and explosive possibly ultrabasic activity. (4) The eruption had ended its most energetic phase by C10 (September 1997). (5) The thermal output from the emplaced flows continued to decline through May 1999 as cooling took place. However, the duration of the energetic, high-*T* Pillan eruption episode can be roughly constrained between 52 days (assuming a start the day before G8 and an end the day after C9) and 167 days (assuming a start the day after G7 and an end the day before C10). Using similar calculations, the very dark flows observed in the Pillan region must have covered at least 3100 km$^2$ in <83-167 days, thus suggesting areal coverage rates ~19-37 km$^2$ day$^{-1}$.

## 3. Galileo Imaging of Pillan Patera

After discovery of the large dark deposit around Pillan Patera from orbit C10 SSI data, it was decided that a high-resolution mosaic of these potentially ultrabasic deposits should be obtained during the Io phase of GEM. Orbit I24 (October 1999) was an equatorial flyby of Io and enabled high- and medium-resolution (tens to hundreds of meters per pixel) imaging over several of Io's prominent volcanoes [see *Keszthelyi et al.*, this issue]. Almost all of the I24 images were

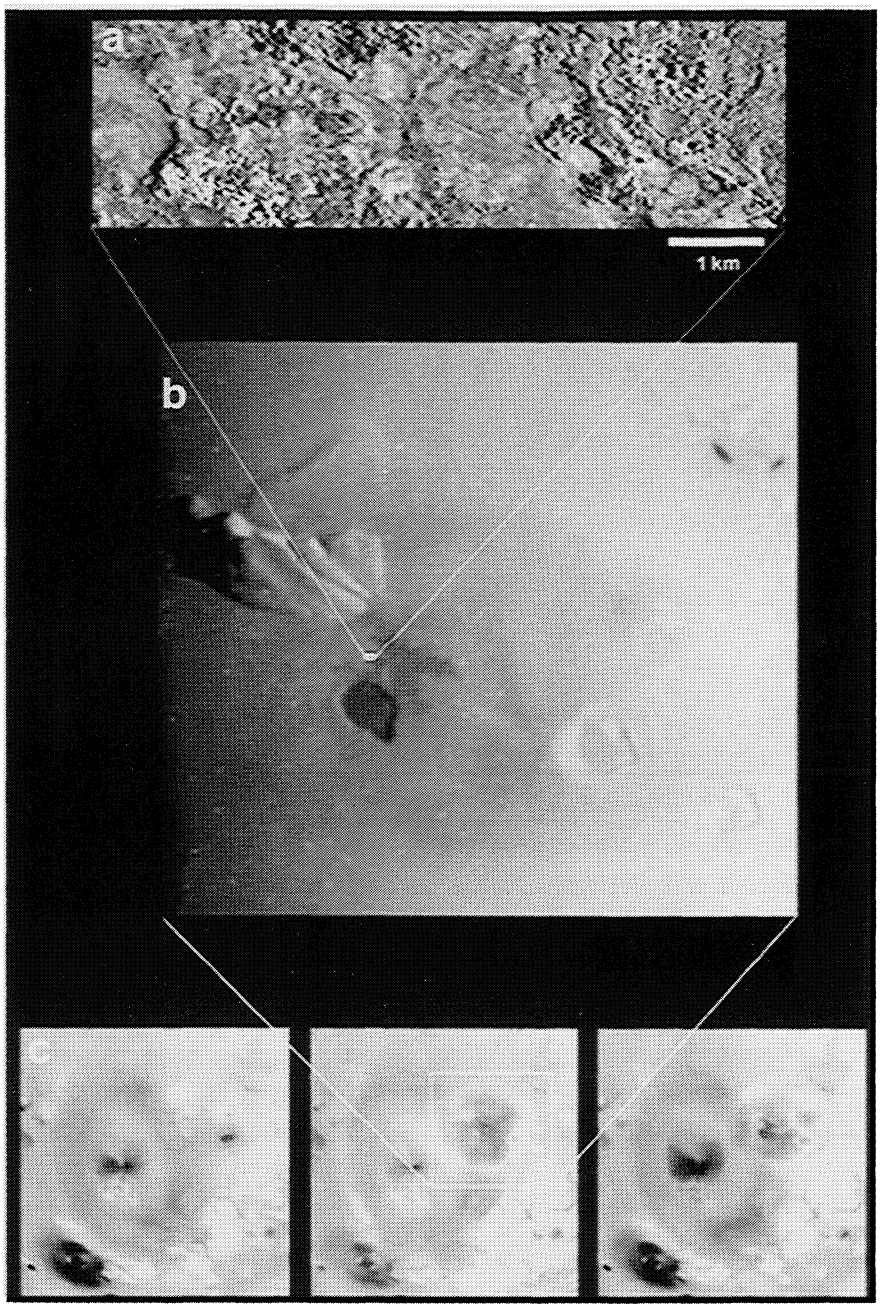


**Figure 2.** Composite image of several Galileo views of Pillan Patera at increasing resolution. (a) Highest-resolution image (9 m pixel$^{-1}$) of Io's surface returned to date showing the complex, rough, domed-and-pitted terrain in the Pillan flow region north of the caldera. (b) An enlarged global-scale (2.6 km pixel$^{-1}$) image of the Pillan region from Galileo orbit E14 (March 1998). (c) Global-scale (5-6 km pixel$^{-1}$) images showing changes in the Pele-Pillan region between April 1997 and July 1999. Modified from Galileo press release PIA02507.

taken using the SSI's 2x2 pixel summation mode with a fast (2.6 s) readout time, which was designed to minimize radiation noise [*McEwen et al.*, 2000]. Radiation models and extrapolations suggested radiation noise in the images taken close to Io would be severe, but the noise was only 20% worse than that typically found at Europa. Unfortunately, the summation mode of the SSI failed during I24, resulting in scrambled images. Because the data scrambling followed an identifiable pattern (the left and right halves of each frame are summed together, but with a 7-pixel horizontal offset of alternate rows of data from the right-hand side [*McEwen et al.*, 2000]), G. Levanas and K. Klaasen of the Jet Propulsion Laboratory developed an algorithm that unscrambled these images using LabVIEW software from National Instruments of Austin, Texas. Thus the images could be partially processed and interpretable mosaics were made.

Figure 2a contains a partial frame of surface materials at Pillan Patera at very high resolution (~9 m pixel$^{-1}$). Figure 3 is the high-resolution (20 m pixel$^{-1}$), unscrambled mosaic of the Pillan materials. Galileo Photopolarimeter-Radiometer (PPR)

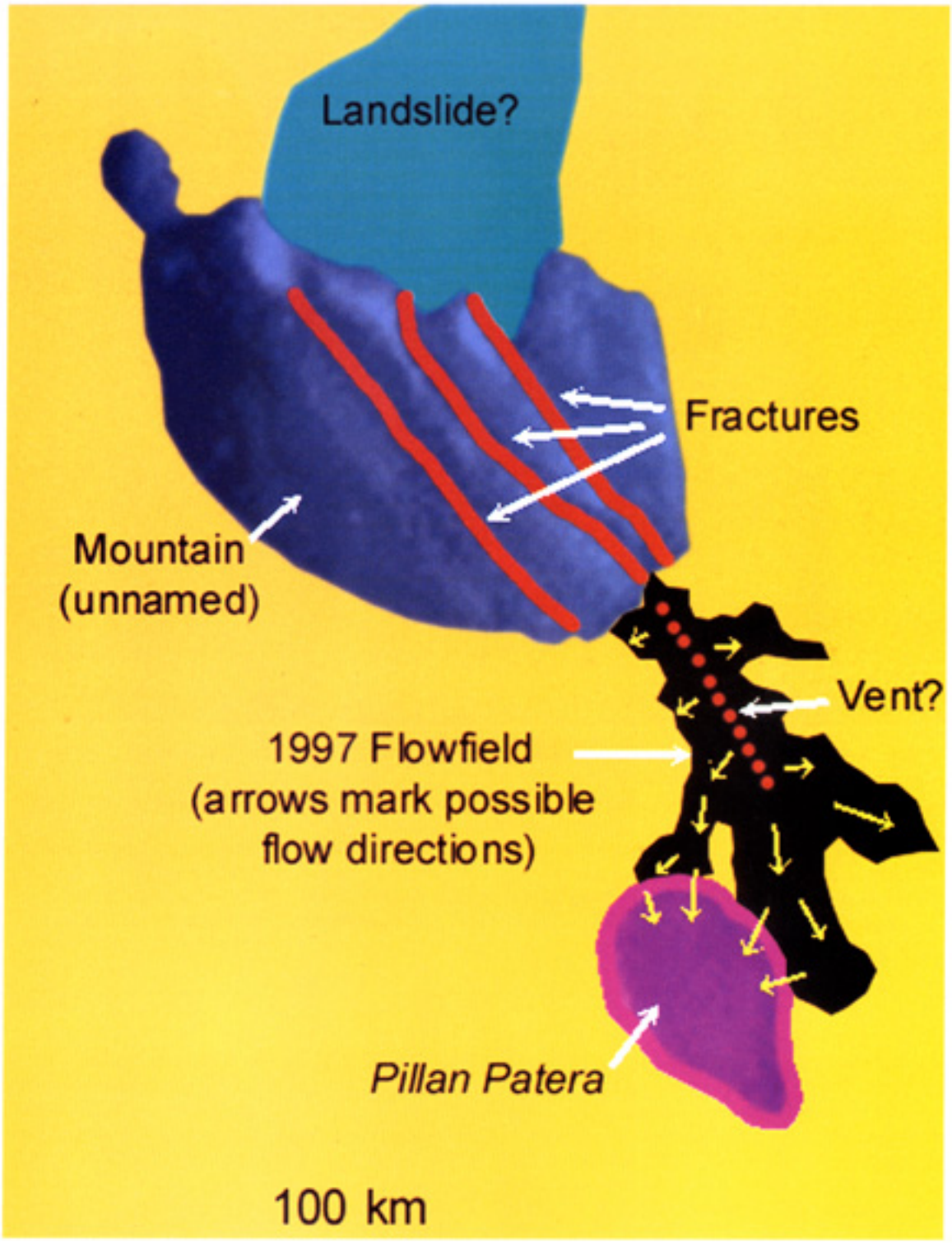


**Plate 1.** Geomorphologic sketch map of the region surrounding Pillan Patera. An extension of a fracture system in an unnamed mountain to the north of the Pillan caldera may have served as a fissure vent for the dark flows from the 1997 eruption. Maximum flow dimensions are at least 60 km long and up to 60 km wide.

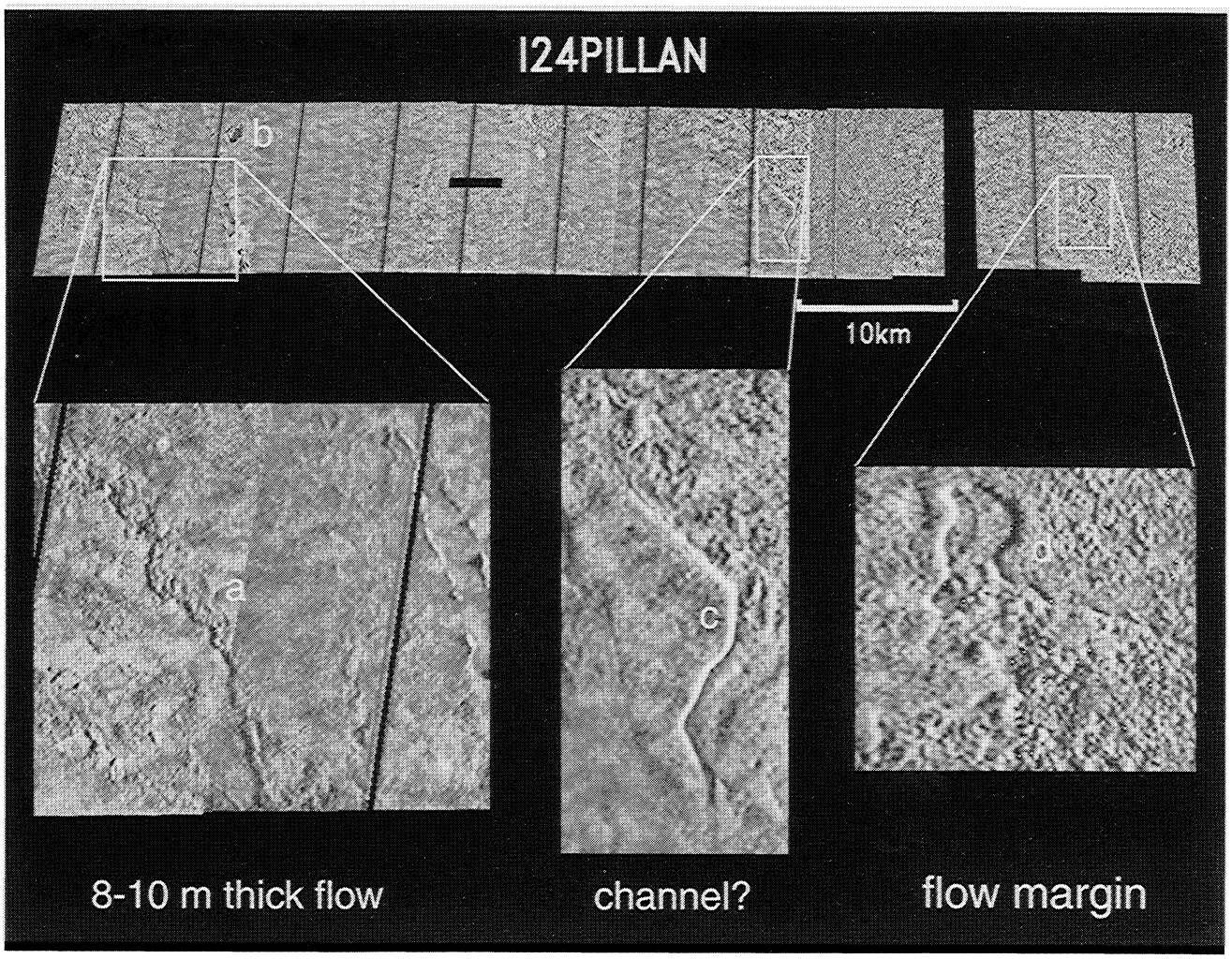


**Figure 3.** High-resolution (20 m pixel$^{-1}$) Galileo mosaic of part of the Pillan flow field resulting from the summer 1997 eruption. (a) The mosaic shows several flow margins, in which shadow measurements indicate a flow thickness of ~8-10 m. (b) A large pit that may be a rootless vent. (c) A sinuous depression that may be a lava channel. (d) A lobe-like flow margin, indicating the distal end of the flow. The rough, domed, and pitted nature of the flow surface is thought to be caused by a fractured lava crust formed during rapid, low-viscosity lava surging, perhaps during turbulent flow emplacement; disruption of the lava flow by explosive interaction with a volatile-rich substrate; or a combination of the above with or without accumulation of pyroclastic materials on the surface. The vertical black bands in each frame are an artifact of the descrambling process applied to Galileo I24 summation mode images. Illumination is from the right, north is to the top.

data indicate that these materials were still warm during orbit I24 [*Spencer et al.*, 2000]. Because we lack context images, the exact location of these high-resolution images is uncertain. However, from spacecraft data this area is probably north of the Pillan caldera in the field of very dark material (see Figure 2 and Plate 1). Figure 2 shows a complex surface of rough and smooth areas at the tens of meters scale, with clusters of pits and domes, perhaps consisting of different types of lava flows or a combination of lavas and pyroclastic materials.

The general morphology of the surface in Figure 3 is similar to that seen in the high-resolution segment of Figure 2; it includes a complex mix of what appear to be flows, channels, pits, domes, and perhaps rafted plates [*McEwen et al.*, 2000]. Several prominent features are also apparent, including (in order from west to east): a distinctive flow margin (Figure 3a), which shadow measurements indicate ranges from ~8.1 to 10.8 m thick; large depressions in the material surface (Figure 3b), which may be rootless vents; a 70-m-wide, >2-km-long sinuous feature (Figure 3c), which may be a wide, open channel, or a flow margin that eroded into the substrate, or a depression between the margins of two flows; and the lobe-like boundary of a rough-textured material in contact with a similarly rough-textured substrate (Figure 3d), which may be the lobe at the end of a flow.

We have compared Figure 3 with available images of terrestrial and planetary lava flows. This comparison is complicated by the degraded quality of the Galileo I24 Pillan mosaic, such that a thorough comparative volcanology analysis cannot be done. Nevertheless, from our analysis we find that the Pillan materials do not obviously resemble other lava flows we have

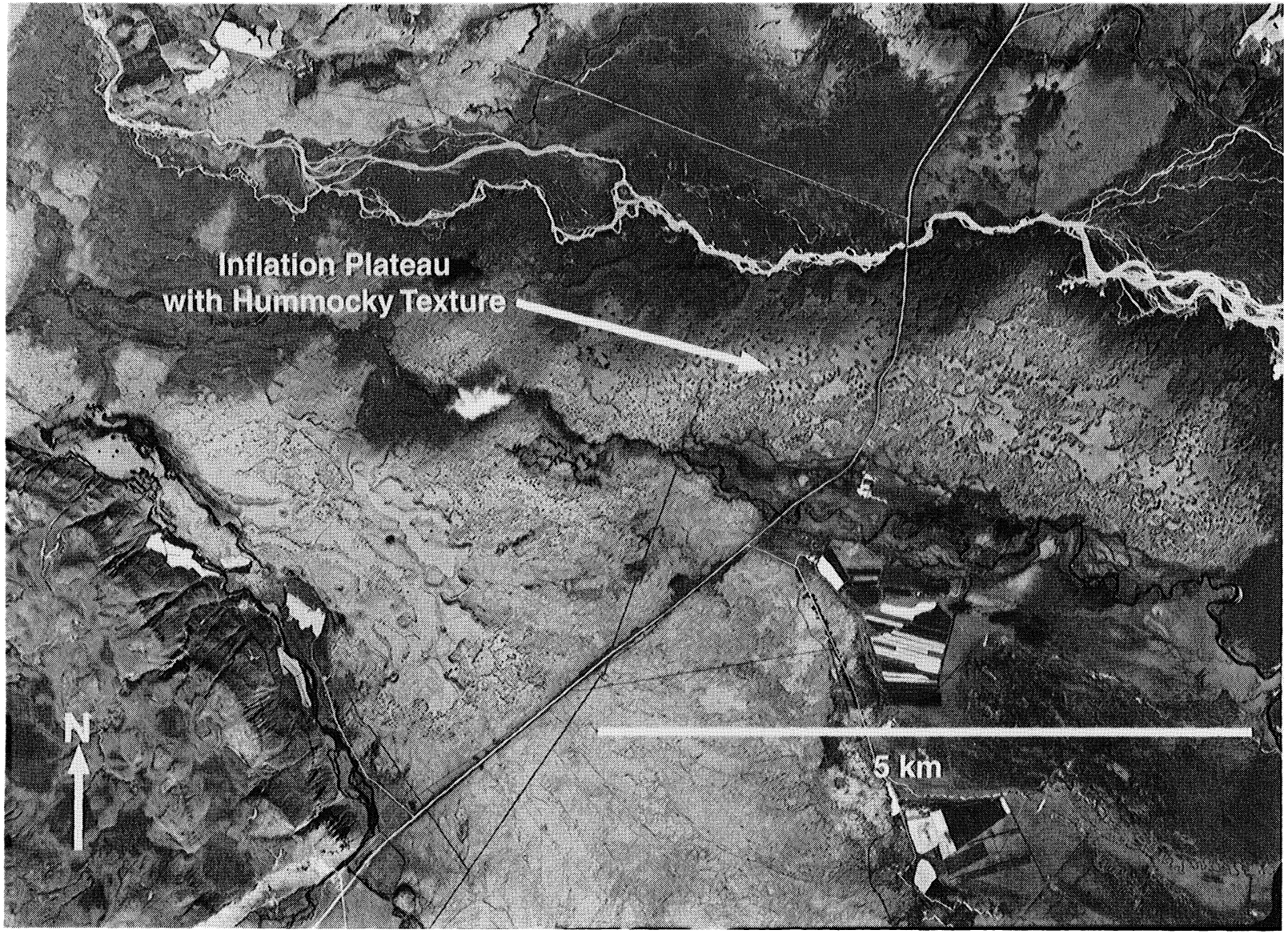


**Figure 4.** Aerial photograph of the SE portion of the Laki, Iceland, flow field from the 1783-1784 eruption. The rough-textured area at center right is an inflation plateau with a hummocky texture. Although this area is the closest analog we have found to the Pillan flows, we think that the Pillan flows are not inflated pahoehoe but rather result from rapid, low-viscosity lava surging, perhaps including turbulent flow emplacement.

studied. The closest analog to the Pillan flow surface that we have been able to find is a rough-textured section of inflated pahoehoe sheet lobes from the 1783-1784 Laki eruption, Iceland (Figure 4). However, the similarities (e.g., mottled flow margins, clusters of pits and domes) appear to be outweighed by the differences (e.g., lack of features that might be tumuli or lava inflation ridges in Figure 3, pits and rises are of different size and shape than those on inflated flows, presence of large plates of material). Thus we think that the Pillan materials are different from typical inflated pahoehoe lava flows. The typical areal coverage rate of Hawaiian inflated pahoehoe flows is ~0.4 $m^2$ $s^{-1}$, or 0.035 $km^2$ $d^{-1}$ [*Mattox et al.*, 1993]. The coverage rate of the pahoehoe sheet lobe in Figure 4 is estimated to be <4 $km^2$ $d^{-1}$, whereas the estimated areal coverage rate of the Roza Member of the Columbia River Flood Basalt Group is estimated to be ~10 $km^2$ $d^{-1}$ [*Thordarson and Self*, 1998]. These values are much less than our estimated areal coverage rate of the Pillan flows (19-37 $km^2$ $d^{-1}$). Furthermore, if the Pillan flows came from ultramafic magma (see section 2), then they likely had a lower viscosity than that of the mafic lavas that form inflated pahoehoe flows. We think that this combination of different eruptive and rheologic characteristics produced the unfamiliar surface morphology.

If the Pillan flows are not inflationary pahoehoe flows, then what are they? The original interpretation we made, as described by *McEwen et al.* [2000], is that the presence of what appear to be rafted plates of rock on the upper flow surface suggests fragmentation of lava crust during rapid lava surges or variations in flow emplacement. If the Pillan lavas were low-viscosity, ultrabasic silicates, as suggested by Galileo data [e.g., *McEwen et al.*, 1998b; *Williams et al.*, 2000a] and if our estimates of large areal coverage rates for the Pillan flows are correct, then we think it likely that the Pillan flows underwent rapid emplacement, perhaps including turbulent flows, which might be expected to produce the observed fragmental, blocky, or disrupted crust. Another interesting point is that the apparent flows in Figure 3 are wide, thin sheet flows rather than channelized flows. Wide sheet-like flows fed by preferred pathways (lava channels or tubes) have been described in terrestrial komatiite flows in Western Australia [*Hill et al.*, 1990, 1995; *Perring et al.*, 1995], although they lack rough upper surfaces. The channelization of lava would be expected over rough topography, although we currently lack a good regional resolution (~200 m $pixel^{-1}$) image to constrain the general topography, the distance from the lava source, etc., of the terrain around Pillan.

An alternative explanation for the rough flow surface in Figure 3 is that it might be due to fragmentation of the flow by degassing or disruption of the lava flow by explosive interaction with a volatile-rich substrate. The presence of the large plume during the Pillan eruption suggests either that the ultrabasic magma was volatile-rich or that the volatile-poor magma was becoming volatile-rich through interaction with volatile-rich surroundings. In either case, volatile-rich lavas should undergo degassing during emplacement, which has implications for flow emplacement, which we discuss in the next section. Finally, it has been suggested that the dark Pillan flows might not be lava flows but rather could be pyroclastic flows. Pyroclastic flows on Io were suggested during the Voyager data analysis [*Kieffer*, 1982], and there has been more recent modeling of their emplacement [e.g., *Smythe et al.*, 2000]. They are hard to envision on airless Io, and we doubt that they would produce flows with a morphology similar to that seen in Figure 3. Furthermore, the Galileo thermal data are inconsistent with pyroclastic flows: instead of a steadily cooling surface (typical of rapidly emplaced pyroclastic flows), we see a relatively protracted eruption with multiple hot spots. Thus our preferred interpretation of the Pillan materials is that they are lava flows of ultrabasic composition, a hypothesis which we will test with modeling.

## 4. Komatiite Analog and Modeling

On the basis of the inferred magma liquidus temperature of the 1997 Pillan eruption (~1870 K or ~1600°C [*Davies et al.*, this issue]) and the identification of orthopyroxene in the dark Pillan deposits [*McEwen et al.*, 1998b; *Geissler et al.*, 1999], *Williams et al.* [2000a] identified a possible terrestrial komatiite analog composition to the inferred Ionian ultrabasic materials. Komatiites are terrestrial, magnesium-rich ultrabasic volcanic rocks and occur as altered or metamorphosed greenstones found almost exclusively in Precambrian terrains [*Arndt and Nisbet,* 1982]. Although there is an ongoing debate about the maximum MgO contents [e.g., *Arndt and Nisbet,* 1982; *Nisbet et al.*, 1993], eruption temperatures [e.g., *Parman et al.*, 1997], style of flow emplacement [*Huppert and Sparks*, 1985; *Hill et al.*, 1995; *Cas et al.*, 1999; *Dann*, 2000], and original volatile contents of komatiite magmas [*Arndt et al.*, 1998; *Grove et al.*, 1999; *Beresford et al.*, 2000], the original interpretation based on the geochemistry of komatiites (Table 2) suggests that they had high MgO contents (~18-32% [*Arndt and Nisbet*, 1982]) and thus are inferred to have had low dynamic viscosities (~0.1-2 Pa s), high liquidus temperatures (~1360-1640°C), and great potential for turbulent flow and for the production of thermal erosion channels [*Huppert et al.,* 1984; *Huppert and Sparks,* 1985; *Jarvis,* 1995; *Williams et al.,* 1998]. *Williams et al.* [2000a] found that the ~3.2-3.5 Ga [*Wilson and Carlson,* 1989; *Lopez-Martinez et al.,* 1992] komatiite flows in the Commondale greenstone belt of South Africa, which contain rare orthopyroxene spinifex crystals and which are inferred to have erupted from hot (~1880 K, 1610°C), Mg-rich (~31% MgO) lavas, are the closest analog to Ionian ultrabasic materials.

From the analysis of Galileo data, we can list the following constraints on modeling ultrabasic flow emplacement at Pillan.

1. The Galileo SSI/NIMS temperature-area data for the 1997 Pillan eruption in the *Davies et al.* [this issue] silicate cooling model require a minimum magma eruption temperature of 1870 K (1597°C). This value is very close to the liquidus temperature of the Commondale komatiite/Io analog composition of 1884 K (1611°C [*Williams et al.*, 2000a]), as calculated by the igneous petrology program MELTS [*Ghiorso and Sack*, 1995]. Given the identification of orthopyroxene in the Pillan deposits [*McEwen et al.*, 2000] and recognizing that most magmas erupt below their liquidus temperatures (in which the two-temperature-area model fit provides only a lower limit on magmas liquidus temperature), we believe that the Commondale composition is a useful analog. We can evaluate flow emplacement with this composition for the range of eruption temperatures consistent with Galileo data.

2. The minimum thickness of the 1997 Pillan flows (8.1-10.8 m) constrains the initial thickness of the Pillan flows. Assuming that these values are typical of the Pillan flows and,

**Table 2.** Inferred Liquid Compositions and Physical Properties for Several Komatiitic and Basaltic Lavas[a]

| Component | Commondale Komatiite | Kambalda Komatiite | Barberton Komatiite | Cape Smith Komatiitic Basalt | Low-$TiO_2$ Lunar Mare Basalt | Terrestrial Tholeiitic Basalt |
|---|---|---|---|---|---|---|
| $SiO_2$ | 49.8 | 45.0 | 47.9 | 46.9 | 43.6 | 50.9 |
| $TiO_2$ | 0.1 | 0.3 | 0.4 | 0.6 | 2.6 | 1.7 |
| $Al_2O_3$ | 7.9 | 5.6 | 4.1 | 9.8 | 7.9 | 14.6 |
| $Fe_2O_3$ | 0.5 | 1.4 | 1.9 | - | - | - |
| FeO | 4.8 | 9.2 | 9.7 | 14.4 | 21.7 | 14.6 |
| MnO | 0.1 | 0.2 | 0.2 | 0.3 | 0.3 | - |
| MgO | 30.9 | 32.0 | 27.5 | 18.9 | 14.9 | 4.8 |
| CaO | 5.2 | 5.3 | 7.5 | 8.6 | 8.3 | 8.7 |
| $Na_2O$ | 0.4 | 0.6 | 0.2 | 0.3 | 0.2 | 3.1 |
| $K_2O$ | 0.01 | 0.03 | 0.02 | 0.05 | 0.05 | 0.8 |
| $T_{liq}$, °C | 1611 | 1638 | 1556 | 1419 | 1440 | 1160 |
| $T_{sol}$, °C | 1170 | 1170 | 1170 | 1150 | 1150 | 1080 |
| ρ at $T_{liq}$, kg $m^{-3}$ | 2680 | 2770 | 2760 | 2800 | 2900 | 2750 |
| $c$, J $kg^{-1}$ °$C^{-1}$ | 1780 | 1790 | 1740 | 1640 | 1570 | 1480 |
| μ at $T_{liq}$, Pa $s^{-1}$ | 0.22 | 0.08 | 0.20 | 0.74 | 0.40 | 86 |
| $L$ at $T_{liq}$, J $kg^{-1}$ | 6.84E+05 | 6.97E+05 | 6.58E+05 | 5.96E+05 | 6.06E+05 | 5.37E+05 |
| $k$ at $T_{liq}$, J $m^{-1}$ $s^{-1}$ °$C^{-1}$ | 0.4 | 0.4 | 0.4 | 0.5 | 0.5 | 0.7 |
| $h$, m | 10 | 10 | 10 | 10 | 10 | 10 |
| $u$ at $T_{liq}$, m $s^{-1}$ | 4.6 | 4.8 | 4.5 | 3.9 | 4.2[b] | 1.7 |
| $Re$ at $T_{liq}$ | 5.74E+05 | 1.74E+06 | 6.31E+05 | 1.46E+05 | 3.09E+05[b] | 5.50E+02 |
| $Pr$ at $T_{liq}$ | 1.0E+03 | 3.8E+02 | 8.4E+02 | 2.6E+03 | 1.3E+03[b] | 1.9E+05 |
| $h_T$ at $T_{liq}$, J $m^{-1}$ $s^{-1}$ °$C^{-1}$ | 260 | 396 | 277 | 172 | 217[b] | N/A |
| $u_{mb}$ at $T_{liq}$, m $d^{-1}$ | 1.1 | 1.7 | 1.0 | 0.52 | 0.24[b] | N/A |
| Composition location | South Africa | Western Australia | South Africa | Cape Smith Belt, Canada | Ap. 12 Sample 12002 | CRB, Washington |
| Reference[c] | 1 | 2 | 3 | 4 | 5 | 6 |

[a]$T_{liq}$, liquidus temperature; $T_{sol}$, solidus temperature; ρ, density; $c$, specific heat; μ, dynamic viscosity; $L$, heat of fusion; $k$, thermal conductivity; $h$, flow thickness; $u$, flow velocity; $Re$, Reynolds number, $Pr$, Prandtl number, $h_T$, convective heat transfer coefficient; $u_{mb}$, thermal erosion rate of consolidated basalt; N/A, not applicable for nonturbulent flows. Read 6.84E+05 and 6.84 x $10^5$.

[b]If erupted on Earth.

[c]1, *Wilson and Carlson* [1989]; 2, Adapted from *Lesher and Arndt* [1995]; 3, *Viljoen et al.* [1983]; 4, *Barnes et al.* [1982]; 5, *Walker et al.* [1976]; 6, *Murase and McBirney* [1973].

for simplicity, assuming a constant flow rate and recognizing that lava flows under such conditions will increase in thickness as velocity decreases due to cooling and crystallization, the initial flow thickness must have been <8 m.

3. The presence of the 140-km-high eruption plume and the widespread pyroclastic deposits associated with the 1997 Pillan event suggests that either the magma was volatile-rich, or significant lava-substrate interactions were occurring [*Kieffer et al.*, 2000; *Milazzo et al.*, this issue]. *Williams et al.* [2000a] showed that $SO_2$ bubbles in the magma would affect the thermal and rheological properties of an Ionian ultrabasic lava, increasing lava viscosity and decreasing maximum potential flow distance and thermal erosion potential. The effects were greater for increasing fractions of volatiles in the lava. Although we cannot quantify the bubble fraction/volume in the Pillan lavas, we assume a reasonably high vesicle content in the lava (e.g., 40%) for our modeling.

4. In the I24 Pillan high-resolution mosaic the substrate material in contact with the flows has a morphology similar to that for the flows. Although a substrate of a different composition cannot be ruled out, it is reasonable to assume that the Pillan flows were emplaced over earlier flows of a similar composition. Another likely possibility is that a dusting of some sulfurous materials (e.g., $S_8$ particles from Pele, or $SO_2$ frosts from the vents to the east) covers earlier flows. One might expect that a hot silicate flow coming into contact with cold sulfurous materials would cause such material to vaporize and quickly be lost (vaporization rates ~45 cm/100 days [*Milazzo et al.*, this issue]), perhaps resulting in flow front plumes such as those observed at Prometheus [*Kieffer et al.*, 2000]. On the other hand, on at least three occasions in Iceland, lavas have flowed over snow-covered ground without melting the snow (T. Thordarson, personal communication, 2001). For the current model runs, we will for simplicity assume flow over a substrate with the same ultrabasic composition and physical properties.

5. The morphology of the Pillan flows in the I24 mosaic resembles that of the edge of a lobed sheet flow rather than a narrow channelized flow. Even so, in the interests of generality we choose to model lava emplacement using convective heat transfer coefficients for both sheet flows and for channel flows (see Appendix A).

## 5. Results

Tables 2 and 3 give the starting lava composition and the important physical properties of our model. The physics of our lava emplacement and thermal erosion model as adapted for

**Table 3.** Input Values for Modeling Ultramafic Lava Emplacement on Io

| Parameter | Io |
|---|---|
| Lava composition (Table 2) | Commondale komatiite |
| Eruption temperature, °C | 1600, 1560 |
| Liquidus temperature, °C | 1611 |
| Solidus temperature, °C | 1170 |
| Initial flow thickness, m | 7.5 |
| Emplacement environment | vacuum |
| Ambient temperature, °C | -138 |
| Heat loss off of upper surface | radiation |
| Heat transfer mode | channel flow, sheet flow |
| Crystallizing phases | 90% olivine, 10% Opx |
| Substrate composition | Commondale komatiite |
| Substrate slope | 0.1° |
| Gravity, m $s^{-2}$ | 1.797 |

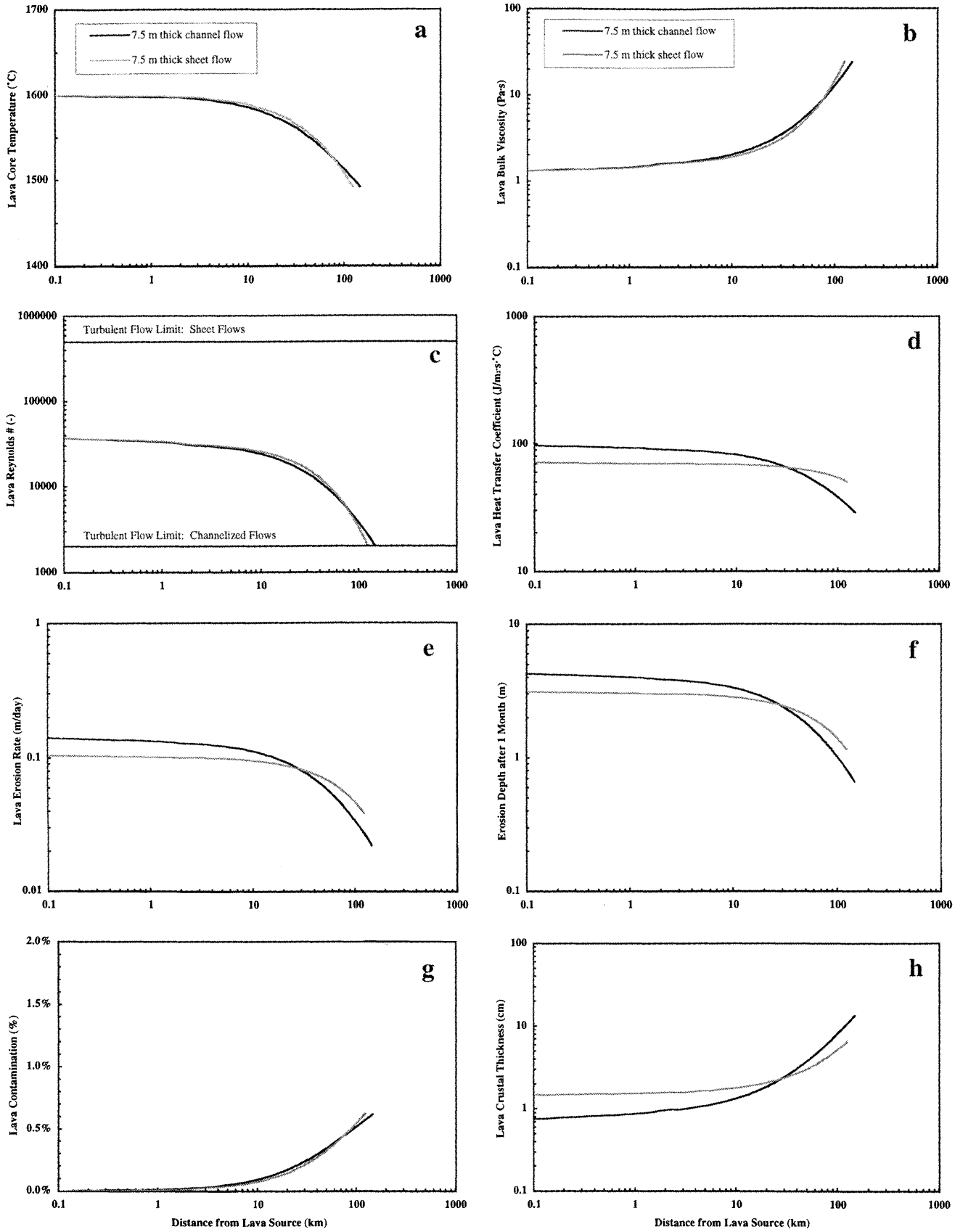


**Figure 5.** Model results for the emplacement of initially 7.5 m thick ultrabasic lava flows over ultrabasic substrate on Io. Flow emplacement assessed using heat transfer coefficients for both channelized and sheet flows. Ground slopes assumed to be 0.1°. All graphs are plotted relative to distance from source (km). (a) Lava interior temperature. (b) Lava bulk viscosity. (c) Lava Reynolds number. (d) Lava heat transfer coefficient. (e) Lava thermal erosion rate. (f) Erosion depth of substrate after one month for flow. (g) Degree of lava contamination by substrate. (h) Lava crustal thickness.

**Table 4.** Model Results for the Emplacement of Ionian Ultrabasic Lava Flows Over Ultrabasic Substrate

| Property | Undercooled Sheet Flow | Subliquidus Sheet Flow | Undercooled Channelized Flow | Subliquidus Channelized Flow |
|---|---|---|---|---|
| Lava eruption temperature, °C | 1560 | 1600 | 1560 | 1600 |
| Initial Reynolds number | 17,700 | 36,800 | 17,700 | 36,800 |
| Flow regime upon eruption | laminar | laminar | turbulent | turbulent |
| Maximum flow distance,[a] km | 50 | 120 | 80 | 150 |
| Maximum flow thickness,[a] m | 9.4 | 10.1 | 9.4 | 10.1 |
| Maximum erosion rate,[b] m $d^{-1}$ | 0.08 | 0.10 | 0.09 | 0.14 |
| Maximum erosion depth after 1 week,[b] m | 0.56 | 0.73 | 0.63 | 0.99 |
| Maximum contamination,[a] % | 0.26 | 0.62 | 0.26 | 0.62 |
| Maximum crustal thickness,[a] cm | 5.4 | 6.4 | 10 | 13 |

[a]Cut off at $Re = 2000$.
[b]At vent.

Io are given by *Williams et al.* [2000a] (see note about heat transfer coefficients in Appendix A). If our assumptions are valid, then our modeling results (Figure 5 and Table 4) show that an initially 7.5-m-thick ultrabasic channelized flow could have traveled almost 150 km as a turbulent flow, assuming a flat, unobstructed surface. In contrast, a comparable sheet flow could have traveled almost 120 km, but as a laminar flow. Turbulent sheet flows require much higher Reynolds numbers ($Re$ > 500,000) than turbulent channelized flows ($Re$ > 2,000) [e.g., *Incropera and DeWitt*, 1990]. These flow distances are theoretical maximums; in reality, topographic obstacles, variations in flow rate, rheological effects of entrained surface crust, and other factors should reduce the actual flow distances attained. For example, an initially 7.5-m-thick, undercooled ($T_0$ = 1560°C) ultrabasic flow that contained ~12% crystals upon eruption would have had a higher bulk viscosity and lower Reynolds number, resulting in a maximum potential flow distance ~50-80 km, depending upon whether it was a sheet flow or channelized flow and all else equal. Given the wide range of unknown or poorly know variables, our model results are remarkably consistent with the measured maximum lengths of the 1997 Pillan flows (~60 km). The flow thicknesses at these modeled flow distances given above are ~9 m, which are also consistent with our measurements from the Galileo I24 Pillan images.

Previous results [*Williams et al.*, 1998, 1999, 2000b] showed that thermal erosion rates for a lava flow over a consolidated substrate of the same composition tend to be low (~0.1 m $d^{-1}$), such that long-duration eruptions (months) are required to produced deep (tens of meters) channels. This supposition was confirmed by the observations of *Kauahikaua et al.* [1998], who noted that low erosion rates (~0.1 m $d^{-1}$) occurred for tholeiitic basalt lava over basalt substrate in active Hawaiian lava tubes. They further noted that continuous eruption of basalt lava in tubes for weeks to months may have caused erosion of >20 m of basaltic substrate. Our model results for the 1997 Pillan flows suggest very low maximum erosion rates (0.05-0.1 m $d^{-1}$), which for the inferred maximum eruption duration (167 days) results in maximum potential erosion of <20 m. This value is below the resolution limit of the I24 Pillan images, so that no clear examples of thermal erosion should be visible, and none are observed. In addition, if the Ionian ultrabasic lava were to come into contact with a layer of $SO_2$ frost or sulfur pyroclastics overlying previously emplaced flows, then considerable energy would be expended melting or sublimating these materials [*Milazzo et al.*, this issue], leaving less heat energy available for thermal erosion. For example, our preliminary calculations indicate that the energy required to sublimate $SO_2$ frost at an Ionian surface temperature of −138°C is 1.33 x $10^9$ J $m^{-3}$, which is ~16% of the energy to melt the ultrabasic lava at that temperature (8.07 x $10^9$ J $m^{-3}$).

## 6. Discussion

### 6.1. Comparison With Terrestrial Komatiite Flows

It is not possible to directly compare potentially ultrabasic Ionian flows with terrestrial komatiite flows because komatiite flow morphologies must be inferred from weathered, metamorphosed, and/or structurally deformed outcrops, drill cores, or underground exposures in mines. However, from studies of these materials, some general ideas about the emplacement of terrestrial komatiites have been made [e.g., *Huppert and Sparks*, 1985; *Hill et al.*, 1990, 1995]. Komatiite lava flows appear to have been emplaced as fields of multiple flow units indicative of episodic emplacement. They appear to have had a wide variety of facies, including flood or sheet flows, sheet flows fed by a distinguishable and dominant central preferred pathway (i.e., channelized sheet flow [*Lesher et al.*, 1984]), confined flows (i.e., lava channels/tubes), compound massive and lobed flows, pillowed flows, and ponded flows [*Arndt et al.*, 1979; *Hill et al.*, 1995], as well as subvolcanic intrusives [*Parman et al.*, 1997]. Flow thicknesses range from tens of centimeters to tens of meters. All terrestrial komatiite flows appear to have been emplaced in subaqueous environments, and most are inferred to have been emplaced on the deep ocean floor. Pyroclastic komatiitic rocks are rare, and those komatiitic deposits that might be of explosive origin are thought to have been emplaced either in shallow water environments [*Saverikko*, 1990] or emplaced during volatile-rich eruptions [e.g., *Gélinas et al.*, 1977; *Schaefer and Morton*, 1991]. Turbulent, channelized flow has been the conventional paradigm for komatiitic lava emplacement [*Huppert et al.*, 1984; *Huppert and Sparks*, 1985; *Jarvis*, 1995], although more recent work suggests that laminar flow, insulating transport, and inflation (i.e., injection of lava underneath a crust causing a slow expansion of the flow) may have occurred in many komatiite eruptions [*Hill et al.*, 1995; *Perring et al.*, 1995; *Hill and Perring*, 1996; *Cas et al.*, 1999; *Dann*, 2000].

On the basis of our study of the 1997 Pillan eruption and the resulting deposits, the following points can be made.

1. The large plume and extensive pyroclastic deposit produced by the 1997 Pillan event suggest that volatile-induced

explosive eruptions or volatile-substrate interactions play a significant role in ultrabasic eruptions on Io, and a much greater role than explosive komatiitic volcanism played on Earth. The other convincing examples of high-*T* eruptions on Io (Kanehekili? [*Veeder et al.*, 1994], Pele [*Lopes et al.*, this issue] and Tvashtar [*Wilson and Head*, this issue; D.S. Acton, unpublished manuscript, 2001]) are associated with either plumes or lava fountains. This is due in part to the environmental differences between Earth and Io; most terrestrial komatiite eruptions are thought to have been submarine, in which the higher pressures at the ocean floor would suppress volatile exsolution and explosive fragmentation. This is also probably due to the greater magma volatile contents and/or greater magma-volatile interaction during ascent through the crust and/or flow on the surface on Io; most early workers considered terrestrial komatiites to be anhydrous [cf. *Stone et al.*, 1997; *Grove et al.*, 1999]. On the other hand, recent studies suggest some terrestrial komatiites were vesicle-rich (up to 30% [*Beresford et al.*, 2000]), and may have undergone volatile degassing during emplacement. Degassing would have had an effect on lava rheology, causing undercooling, rapid nucleation, and crystallization. These effects would have increased bulk viscosity, decreased Reynolds number, and thus decreased potential flow distances and reduced thermal erosion rates.

2. The rough, fractured, domed, and pitted nature of the Pillan flows is suggestive of rapid lava surges or variations in flow rate, perhaps from turbulent to laminar flow emplacement, in which a stable insulating crust was continuously disrupted [*Keszthelyi and Self*, 1998]. Terrestrial komatiites provide equivocal clues as to the nature of their original crusts. Most komatiites consist of several textural zones, including a thin (few centimeters) upper chill margin, a zone of randomly oriented olivine or clinopyroxene spinifex crystals, a zone of larger, roughly vertically oriented spinifex crystals, and several zones of more typical equant olivine cumulate crystals that may or may not overlie a lower chill margin [*Pyke et al.*, 1973; *Hill et al.*, 1990]. Spinifex and cumulate zones in komatiite flows are thought to form after ponding, while the hot komatiite may still be convecting underneath [*Turner et al.*, 1986]. Thus if the thin upper chill margin is assumed to be the "crust" present during flow, then its apparently smooth and unfractured surface may be more consistent with slow, inflationary, pahoehoe-style emplacement rather than fast, turbulent emplacement. Some komatiitic flows do have flow top breccias, which have been interpreted as the fragmental upper crusts expected to occur during turbulent flow [*Lesher and Thibert*, 2001].

3. The morphology of the flows in the Pillan images appears to be consistent with a relatively distal part of a lobed flow. However, we have not seen high-resolution images of a more proximal (to the source) region of the Pillan flow field, where deep lava channel/tubes should occur. It is our opinion that while the Pillan flows may resemble compound lava flows (but not inflated pahoehoe), the Pillan flows are most likely lava flows emplaced by rapid, perhaps turbulent, ultramafic lava surges. Although there definitely appears to be evidence of slow, inflationary silicate flow emplacement on Io (e.g., Amirani, Prometheus [see *Keszthelyi et al.*, this issue]), and some Galileo data support insulated emplacement at Pillan (i.e., the C10 dual hot spots, interpreted by *McEwen et al.* [1998a] as the vent and toe of a long dark flow), we think the Pillan flows are something different. However, we think that the range of compositions and styles of lava emplacement on Io are likely as broad as the styles of emplacement of terrestrial komatiites. Future Galileo Io encounters tentatively planned for late 2001 and early 2002 will include imaging of both the proximal and distal segments of potentially ultrabasic flow fields (e.g., Tvashtar, Masubi, Kanehekili, and Pillan) to determine how diverse ultrabasic flow morphology may be.

### 6.2. Flow Rate of Pillan C9 Eruption

Existing information can be used to estimate flow rates during the 1997 Pillan eruption. Galileo SSI and NIMS data from repeated flybys of Io in 1997 suggest that the duration of the high-T Pillan event was 52-167 days. SSI images of Pillan taken during GEM show the areal extent of the dark flows at Pillan associated with the 1997 high-*T* eruption episode to be ~3100 km$^2$. Shadow measurements of the flow margins indicate that the lava flow thicknesses are ~8.1-10.8 m. These results yield an areal coverage rate or (two-dimensional) flow rate of ~215-690 m$^2$ s$^{-1}$, and a volumetric flow rate of ~1740 to ~7450 m$^3$ s$^{-1}$. These rates are greater than those for the (1984) Mauna Loa eruption (~700-800 m$^3$ s$^{-1}$) and are comparable to the (1783) Laki eruption (3000-8000 m$^3$ s$^{-1}$) and the Roza Columbia River flood basalt flows (4000 m$^3$ s$^{-1}$ [*Thordarson and Self*, 1993, 1998]). However, these rates are an order of magnitude smaller than that estimated for Martian flood lavas [*Keszthelyi et al.*, 2000]. Note that this only refers to the dark flows and does not include the larger diffuse pyroclastic deposit.

## 7. Summary

We have analyzed Galileo data and new numerical modeling results to study the nature of the summer 1997 high-temperature eruption at Pillan Patera on Io. Galileo SSI and NIMS data indicate that this eruption (now defined as of "Pillanian" eruption style [see *Keszthelyi et al.*, this issue]) included a large (140-km-high) plume that deposited dark, possibly orthopyroxene-rich material over an area >125,000 km$^2$, with minimum temperatures at the height of the eruption ~1600°C (consistent with ultrabasic materials), followed by emplacement of a series of dark flows to the north of the caldera [*McEwen et al.*, 1998b]. This high-*T* eruption episode had a duration of ~52-167 days and is marked by an increase in thermal emission during May 1997, a peak around July 1997, and a decrease in emission by September 1997. Galileo high-resolution (20 m pixel$^{-1}$) images of part of the Pillan flow field show a widespread, fractured, domed, and pitted surface unlike those seen on terrestrial lava flows at these scales, perhaps indicative of (1) a fractured lava crust formed during rapid lava surging, perhaps during turbulent flow emplacement; (2) disruption of the lava flow by explosive interaction with a volatile-rich substrate; or (3) a combination of 1 and 2 with or without accumulation of pyroclastic materials on the surface. One >2-km-long, ~70-m-wide sinuous feature (lava channel?) and several well-developed flow lobes are visible, indicating that this region may be relatively distal to the source of the flow field. Shadow measurements at flow margins indicate a flow thickness of ~8-10 m.

Using the komatiite lava analog composition of *Williams et al.* [2000a] and additional constraints from Galileo data (e.g., flow thickness, likely volatile-rich lava, ultrabasic substrate composition), we have modeled the emplacement of pu-

tative ultrabasic flows from the 1997 Pillan eruption. Our results suggest that either laminar sheet flows or turbulent channelized flows could have traveled <50-150 km over a flat, unobstructed surface. These distances are consistent with the length of the Pillan flow field (~60 km) estimated from Galileo images. Our modeling suggests that low thermal erosion rates (<0.1 m $d^{-1}$) occurred for flow over an ultrabasic substrate and that for the known eruption duration, modeled thermal erosion depths (<20 m) are below the limit of resolution of the images, such that obvious evidence of thermal erosion should not be apparent. One large sinuous feature in the Pillan mosaic may be a lava channel, although the image degradation makes a positive identification uncertain. However, deep (>20 m) channels would be expected more proximal to the source of the Pillan flow field. Given the eruption duration, the areal coverage, and the flow thickness of the Pillan flows, we calculate average volumetric flow rates of the Pillan eruption of ~1700-7400 $m^3$ $s^{-1}$. These flow rates are comparable to those for the (1783) Laki eruption (3000-8000 $m^3$ $s^{-1}$) and the Roza flows in the Columbia River Basalt Province [*Thordarson and Self*, 1993, 1998], but are an order of magnitude smaller than the flow rates estimated for the largest Martian flood lavas [*Keszthelyi et al.*, 2000].

The presence of plumes at sites of potentially ultrabasic eruptions on Io suggests that Io's eruption environment (low-gravity, lack of atmosphere) enhances the potential for magma-volatile interactions to play an important role in ultrabasic eruptions on Io, in contrast to the Precambrian Earth where submarine, effusive emplacement was dominant. Future work could focus on obtaining a better understanding of these magma-volatile interactions on Io, as well as obtaining better temperature, compositional, and morphological constraints at localities of inferred ultrabasic eruptions. These will be some of the goals of future Galileo encounters with Io during the extended Galileo millennium mission (GMM) through early 2002.

## Appendix A: Ultrabasic Lava Emplacement and Erosion Model

The emplacement and thermal erosion model for low-viscosity, turbulently flowing, komatiite lavas was first summarized by *Williams et al.* [1998, 1999] and was adapted to study low-viscosity extraterrestrial silicate lava flows erupted on Io [*Williams et al.*, 2000a] and on the Moon [*Williams et al.*, 2000b]. The model used in this work is the same as that given by *Williams et al.* [2000a], except that we have performed model runs using a different heat transfer coefficient. This is discussed below.

*Hulme* [1973] and *Huppert and Sparks* [1985] showed that low-viscosity, turbulently flowing lavas should loose heat to their surroundings primarily by convection. Both used a convective heat transfer coefficient for turbulent pipe flows for fluids with constant physical properties. However, lava flows not only undergo phase changes but also have temperature-dependent physical properties. Thus a more appropriate convective heat transfer coefficient ($h_T$) is desirable, which includes the effect for fluids with temperature-dependent physical properties. Such an expression for turbulent pipe flows [see *Kakaç et al.*, 1987] is given by

$$h_T = \frac{0.027 k_{\mathrm{eff}} Re^{4/5} Pr^{1/3}}{h} \left( \frac{\mu_b}{\mu_g} \right)^{0.14}, \qquad \text{(A1)}$$

in which $k_{\mathrm{eff}}$ is the effective thermal conductivity in the thermal boundary layers at the top and base of the flow, $Re$ is the lava Reynolds number, $Pr$ is the lava Prandtl number, $\mu_b$ is the lava bulk viscosity, $h$ is the lava flow thickness, and $\mu_g$ is the viscosity of the melted substrate. The ratio of the lava bulk viscosity to the viscosity of the melted substrate in (A1) typically has the effect of reducing heat transfer compared to that occurring in fluids with constant fluid physical properties. Equation (A1) is the $h_T$ used by *Williams et al.* [2000a]. To model turbulent and laminar sheet flows in this work, we have used the following expressions [see *Kakaç et al.*, 1987]:

$$h_T = \frac{0.0296 k_{\mathrm{eff}} Re^{4/5} Pr^{1/3}}{h} \left( \frac{\mu_b}{\mu_g} \right)^{0.14} \qquad \text{(A2)}$$

for a turbulent sheet flow ($Re$ limit = 500,000) and

$$h_T = \frac{0.4637 k_{\mathrm{eff}} Re^{1/2} Pr^{1/3}}{h \left[ 1 + (0.0205/Pr)^{2/3} \right]^{1/4}} \left( \frac{\mu_b}{\mu_g} \right)^{0.14} \qquad \text{(A3)}$$

for a laminar sheet flow.

## Notation

| | |
|---|---|
| $h$ | lava flow thickness, m. |
| $h_T$ | lava convective heat transfer coefficient, J $m^{-2}$ $s^{-1}$ °$C^{-1}$. |
| $k_{\mathrm{eff}}$ | lava effective thermal conductivity, J $m^{-1}$ $s^{-1}$ °$C^{-1}$. |
| $\mu_b$ | lava bulk viscosity, Pa $s^{-1}$. |
| $\mu_g$ | substrate melt viscosity, Pa $s^{-1}$. |
| $Pr$ | lava Prandtl number. |
| $Re$ | lava Reynolds number. |
| $T$ | lava temperature, °C. |
| $T_0$ | lava eruption temperature, °C. |

**Acknowledgments.** The authors would like to thank Ken Klaasen and Greg Levanas for developing the program to unscramble the I24 images, and we thank Thorvaldur Thordarson and an anonymous reviewer for very helpful reviews which improved the quality of the manuscript. We would also like to thank Paul Lucey and Sheehan Morrison for their exceptional efforts at assembling this Io Special Section, and the Galileo Project personnel at the Jet Propulsion Laboratory for keeping the spacecraft and instruments working through the Io flybys. A.G.D. is supported by the NASA JSDAP proposal 624-02-0018. D.A.W., L.P.K., and R.G. are supported by grants from the National Aeronautics and Space Administration.

## References

Arndt, N.T., and E.G. Nisbet, *Komatiites*, 526 pp., Allen and Unwin, Concord, Mass., 1982.

Arndt, N.T., D.M. Francis, and A.J. Hynes, The field characteristics and petrology of Archean and Proterozoic komatiites, *Can. Mineral., 17*, 147-163, 1979.

Arndt, N., C. Ginibre, C. Chauvel, F. Albarede, M. Cheadle, C. Herzberg, G. Jenner, Y. Lahaye, Were komatiites wet?, *Geology, 26*, 739-742, 1998.

Barnes, S.J., C.J.A. Coats, and A.J. Naldrett, Petrogenesis of a Proterozoic nickel sulfide-komatiite association: The Katiniq Sill, Ungava, Quebec, *Econ. Geol., 77*, 413-429, 1982.

Beresford, S.W., R.A.F. Cas, D.D. Lambert, and W.E. Stone, Vesicles in thick komatiite lava flows, Kambalda, Western Australia, *J. Geol. Soc. London, 157*, 11-14, 2000.

Cas, R., S. Self, and S. Beresford, The behaviour of the fronts of komatiite lavas in medial to distal settings, *Earth Planet. Sci. Lett., 172*, 127-139, 1999.

Crisp, J., and S. Baloga, Influence of crystallization and entrainment of cooler material on the emplacement of basaltic aa lava flows, *J. Geophys. Res., 99*, 11,819-11,831, 1994.

Dann, J.C., Komatiite flow lobes, inflated sheet flow, and lava tube, 3.5 Ga Komati Formation, Barberton Greenstone Belt, South Africa, *Geol. Soc. Am. Abstr. Programs, 32* (7), A394, 2000.

Davies, A.G., A.S. McEwen, R.M.C. Lopes-Gautier, L. Keszthelyi, R.W. Carlson and W.D. Smythe, Temperature and area constraints of the South Volund volcano on Io from the NIMS and SSI instruments during Galileo G1 orbit, *Geophys. Res. Let., 24*, 2447-2450, 1997.

Davies, A.G., L.P. Keszthelyi, D.A. Williams, C.B. Phillips, A.S. McEwen, R.M.C. Lopes, W.D. Smythe, L.W. Kamp, L.A. Soderblom, and R.W. Carlson, Thermal signature, eruption style, and eruption evolution at Pele and Pillan on Io, *J. Geophys. Res.*, this issue.

Geissler, P.E., A.S. McEwen, L. Keszthelyi, R. Lopes-Gautier, J. Granahan, and D.P. Simonelli, Global color variations on Io, *Icarus, 140*, 265-282, 1999.

Gélinas, L., J. Lajoie, and C. Brooks, The origin and significance of Archean ultramafic volcaniclastics from Spinifex Ridge, La Motte Township, Québec, *Geol. Assoc. Can. Spec. Pap., 16*, 297-309, 1977.

Ghiorso, M.S., and R.O. Sack, Chemical mass transfer in magmatic processes, IV, A revised and internally consistent thermodynamic model for the interpolation and extrapolation of liquid-solid equilibria in magmatic systems at elevated temperatures and pressures, *Contrib. Mineral. Petrol., 119*, 197-212, 1995.

Green, D.H., Genesis of Archean peridotitic magmas and constraints on Archean geothermal gradients and tectonics, *Geology, 3*, 15-18, 1975.

Grove, T.L., S.W. Parman, and J.C. Dann, Conditions of magma generation for Archean komatiites from the Barberton Mountainland, South Africa, in *Mantle Petrology: Field Observations and High Pressure Experimentation: A Tribute to Francis R. (Joe) Boyd, Spec. Publ., Geochem. Soc., 6*, 155-167, 1999.

Harris, A.J.L., A.L. Butterworth, R.W. Carlton, I. Downey, P. Miller, P. Navarro, and D.A. Rothery, Low-cost volcano surveillance from space. Case studies from Etna, Krafla, Cerro Negro, Fogo, Lascar and Erebus, *Bull. Volcanol., 59*, 49-64, 1997.

Harris, A.J.L., J.B. Murray, S.E. Aries, M.A. Davies, L.P. Flynn, M.J. Wooster, R. Wright, and D.A. Rothery, Effusion rate trends at Etna and Krafla and their implications for eruptive mechanisms, *J. Volcanol. Geotherm. Res., 102*, 237-269, 2000.

Hill, R.E.T., and C.S. Perring, The evolution of Archean komatiite flow fields – Are they inflationary sheet flows? (abstract), in *Chapman Conference on Long Lava Flows*, edited by P.W. Whitehead, pp. 18-21, *EGRU Contrib.*, vol. 56, James Cook Univ. of N. Queensl., Townsville, Queensland, Australia, 1996.

Hill, R.E.T., S.J. Barnes, M.J. Gole, and S.E. Dowling, Physical volcanology of komatiites, *Excursion Guideb. 1*, 100 pp., Geol. Soc. Aust., West. Aust. Div., Perth, 1990.

Hill, R. E. T., S.J. Barnes, M.J. Gole, and S.E. Dowling, The volcanology of komatiites as deduced from field relationships in the Norseman-Wiluna greenstone belt, Western Australia, *Lithos, 34*, 159-188, 1995.

Hulme, G., Turbulent lava flows and the formation of lunar sinuous rilles, *Mod. Geol., 4*, 107-117, 1973.

Huppert, H.E., and R.S.J. Sparks, Komatiites, I, Eruption and flow, *J. Petrol., 26*, 694-725, 1985.

Huppert, H.E., R.S.J. Sparks, J.S. Turner, and N.T. Arndt, Emplacement and cooling of komatiite lavas, *Nature, 309*, 19-22, 1984.

Incropera, F.P., and D.P. De Witt, *Fundamentals of Heat and Mass Transfer*, 919pp., John Wiley, New York, 1990.

Jarvis, R.A., On the cross-sectional geometry of thermal erosion channels formed by turbulent lava flows, *J. Geophys. Res., 100*, 10,127-10,140, 1995.

Kakaç, S., R.K. Shah, and W. Aung, *Handbook of Single-Phase Convective Heat Transfer*, John Wiley, New York, 1987.

Kauahikaua, J., K. Cashman, K. Hon, T. Mattox, C. Heliker, M. Mangan, and C. Thornber, Observations on basaltic lava streams in tubes from Kilauea volcano, Hawai'i, *J. Geophys. Res., 103*, 27,303-27,324, 1998.

Keszthelyi, L., and S. Self, Some physical requirements for the emplacement of long basaltic lava flows, *J. Geophys. Res., 103*, 27,447-27,464, 1998.

Keszthelyi, L.P., A.S. McEwen, and T. Thordarson, Terrestrial analogs and thermal models for Martian flood lavas, *J. Geophys. Res., 105*, 15,027-15,050, 2000.

Keszthelyi, L., et al., Imaging of volcanic activity on Jupiter's moon Io by *Galileo* during the Galileo Europa mission and the Galileo millennium mission, *J. Geophys. Res.*, this issue.

Kieffer, S.W., Dynamics and thermodynamics of volcanic eruptions: Implications for the plumes on Io, in *Satellites of Jupiter*, edited by D. Morrison, pp. 647-723, Univ. of Ariz. Press, Tucson, 1982.

Kieffer, S.W., R. Lopes-Gautier, A. McEwen, W. Smythe, L. Keszthelyi, and R. Carlson, Prometheus: Io's wandering plume, *Science, 288*, 1204-1208, 2000.

Lesher, C.M., and N.T. Arndt, REE and Nd geochemistry, petrogenesis, and volcanic evolution of contaminated komatiites at Kambalda, Western Australia, *Lithos, 34*, 127-158, 1995.

Lesher, C.M., and F. Thibert, Stratigraphy and physical volcanology of komatiitic peridotite lava channels, channelized sheet flows, and channelized sheet sills in the Cape Smith Belt, New Quebec, in *Field Guide to Magmatic Fe-Ni-Cu-(PGE) Deposits in the Cape Smith Belt, New Quebec*, edited by C.M. Lesher, Soc. Econ. Geol. Guidebook Ser., El Paso, Tex., in press, 2001.

Lesher, C.M., N.T. Arndt, and D.I. Groves, Genesis of komatiite-associated nickel sulphide deposits at Kambalda, Western Australia: A distal volcanic model, in *Sulphide Deposits in Mafic and Ultramafic Rocks*, edited by D.L. Buchanan and M.J. Jones, pp. 70-80, Inst. of Min. and Metall., London, 1984.

Lopes-Gautier, R., A.G. Davies, R. Carlson, W. Smythe, L. Camp, L. Soderblom, F.E. Leader, R. Mehlman, and the Galileo NIMS Team, Hot spots on Io: Initial results from Galileo's Near-Infrared Mapping Spectrometer, *Geophys. Res. Lett., 24*, 2439-2442, 1997.

Lopes, R.M.C., et al., Io in the near infrared: NIMS results from the Galileo fly-bys in 1999 and 2000, *Journal of Geophysical Research*, this issue.

Lopez-Martinez, M., D. York, and J.A. Hanes, A $^{40}Ar/^{39}Ar$ geochronological study of komatiites and komatiitic basalts from the lower Onverwacht Volcanics, Barberton Mountain Land, South Africa, *Precambrian Res., 57*, 91-119, 1992.

Mattox, T.N., C. Heliker, J. Kauahikaua, and K. Hon, Development of the 1990 Kalapana flow field, Kilauea volcano, Hawaii, *Bull. Volcanol., 55*, 407-413, 1993.

McEwen, A.S., Global color and albedo variations on Io, *Icarus, 73*, 385-426, 1988.

McEwen, A.S., et al., Active volcanism on Io as seen by Galileo SSI, *Icarus, 135*, 181-219, 1998a.

McEwen, A.S., et al., High-temperature silicate volcanism on Jupiter's moon Io, *Science, 281*, 87-90, 1998b.

McEwen, A.S., et al., Galileo at Io: Results from high-resolution imaging, *Science, 288*, 1193-1198, 2000.

Milazzo, M.P., L.P. Keszthelyi, and A.S. McEwen, Observations and initial modeling of lava-$SO_2$ interactions at Prometheus, Io, *J. Geophys. Res.*, this issue.

Murase, T. and A.R. McBirney, Properties of some common igneous rocks and their melts at high temperatures, *Geol. Soc. Am. Bull., 84*, 3563-3592, 1973.

Nisbet, E.G., M.J. Cheadle, N.T. Arndt, and M.J. Bickle, Constraining the potential temperature of the Archaean mantle: A review of the evidence from komatiites, *Lithos, 30*, 291-307, 1993.

Parman, S.W., J.C. Dann, T.L. Grove, and M.J. de Wit, Emplacement conditions of komatiite magmas from the 3.49 Ga Komati Formation,

Barberton Greenstone Belt, South Africa, *Earth Planet. Sci. Lett., 150*, 303-323, 1997.

Perring, C.S., S.J. Barnes, and R.E.T. Hill, The physical volcanology of Archean komatiite sequences from Forrestania, Southern Cross Province, Western Australia, *Lithos, 34,* 189-208, 1995.

Phillips, C.B., Voyager and Galileo views of volcanic resurfacing on Io and the search for geologic activity on Europa, Ph.D. thesis, 269 pp., Univ. of Ariz., Tucson, 2000.

Pinkerton, H., and R.J. Stevenson, Methods of determining the rheological properties of magmas at sub-liquidus temperatures, *J. Volcanol. Geotherm. Res., 53,* 47-66, 1992.

Pyke, D.R., A.J. Naldrett, and O.R. Eckstrand, Archean ultramafic flows in Munro Township, Ontario, *Geol. Soc. Am. Bull., 84,* 955-978, 1973.

Saverikko, M., Komatiitic explosive volcanism and its tectonic setting in Finland, the Fennoscandian (Baltic) Shield, *Bull. Geol. Soc. Finl., 62,* 3-38, 1990.

Schafer, S.J., and P. Morton, Two komatiitic pyroclastic units, Superior Province, northwestern Ontario: Their geology, petrography, and correlation, *Can. J. Earth Sci., 28,* 1455-1470, 1991.

Smythe, W.D., S. Kieffer, L. Camp, R. Lopes, S. Doute, R. Carlson, and the Galileo NIMS Team, Models of volcanic plumes on Io: Results and observations, *Eos Trans. AGU, 81,* (19), Spring Meet. Suppl., S288, 2000.

Spencer, J.R., J.A. Rathbun, L.D. Travis, L.K. Tamppari, L. Barnard, T.Z. Martin, and A.S. McEwen, Io's thermal emission from the Galileo Photopolarimeter-Radiometer, *Science, 288,* 1198-1201, 2000.

Stone, W.E., E. Deloule, M.S. Larson, and C.M. Lesher, Evidence for hydrous high-MgO melts in the Precambrian, *Geology, 25,* 143-146, 1997.

Thordarson, T., and S. Self, The Laki (Skaftár Fires) and Grímsvötn eruptions in 1783-1785, *Bull. Volcanol., 55*, 233-263, 1993.

Thordarson, T., and S. Self, The Roza Member, Columbia River Basalt Group: A gigantic pahoehoe lava flow field formed by endogenous processes?, *J. Geophys. Res., 103,* 27,411-27,445, 1998.

Turner, J.S., H.E. Huppert, and R.S.J. Sparks, Komatiites, II, Experimental and theoretical investigations of post-emplacement cooling and crystallization, *J. Petrol., 27*, 397-437, 1986.

Veeder, G.J., D.L. Matson, T.V. Johnson, D.L. Blaney, and J.D. Goguen, Io's heat flow from infrared radiometry: 1983-1993, *J. Geophys. Res., 99*, 17,095-17,162, 1994.

Viljoen, M.J., R.P. Viljoen, H.S. Smith, and A.J. Erlank, Geological, textural, and geochemical features of komatiitic flows from the Komati Formation, *Spec. Publ. Geol. Soc. S. Afr., 2*, 87-112, 1983.

Walker, D., R.J. Kirkpatrick, J. Longhi, and J.F. Hays, Crystallization history of lunar picritic basalt sample 12002: Phase-equilibria and cooling-rate studies, *Geol. Soc. Am. Bull., 87*, 646-656, 1976.

Williams, D.A., R.C. Kerr, and C.M. Lesher, Emplacement and erosion by Archean komatiite lava flows at Kambalda: Revisited, *J. Geophys. Res., 103*, 27,533-27,549, 1998.

Williams, D.A., R.C. Kerr, and C.M. Lesher, Thermal and fluid dynamics of komatiitic lavas associated with magmatic Ni-Cu-(PGE) sulphide deposits, in *Dynamic Processes in Magmatic Ore Deposits and Their Application in Mineral Exploration*, edited by R.R. Keays et al., *Geol. Assoc. Can. Short Course,* vol. 13, 367-412, Vancouver, B.C., 1999.

Williams, D.A., A.H. Wilson, and R. Greeley, A komatiite analog to potential ultramafic materials on Io, *J. Geophys. Res., 105*, 1671-1684, 2000a.

Williams, D.A., S.A. Fagents, and R. Greeley, A reassessment of the emplacement and erosional potential of turbulent, low-viscosity lavas on the Moon, *J. Geophys. Res., 105,* 20,189-20,206, 2000b.

Wilson, A.H., and R.W. Carlson, A Sm-Nd and Pb isotopic study of Archaean greenstone belts in the southern Kaapvaal craton, South Africa, *Earth Planet. Sci. Lett., 96*, 89-105, 1989.

Wilson, L., and J.W. Head III, Lava fountains from the 1999 Tvashtar Catena fissure eruption on Io: Implications for dike emplacement mechanisms, eruption rates, and crustal structure, *J. Geophys. Res.*, this issue.

---

A.G. Davies, Jet Propulsion Laboratory, California Institute of Technology, MS 183-601, 4800 Oak Grove Drive, Pasadena, CA 91109. (Ashley.Davies@jpl.nasa.gov)

R. Greeley and D.A. Williams, Department of Geological Sciences, Arizona State University, Box 871404, Tempe, AZ 85287. (greeley@asu.edu; williams@dione.la.asu.edu)

L.P. Keszthelyi, Lunar and Planetary Laboratory, University of Arizona, 1629 East University Blvd., Tucson, AZ 85721. (lpk@pirl.lpl.arizona.edu)

(Received July 28, 2000; revised March 1, 2001;
accepted March 16, 2001.)